Synthesis of bisimidazolium-ionic liquids: charaterization, thermal stability and application to bentonite application

B. Makhoukhi, D Villemin, M. A. Didi

Available online at www.sciencedirect.com

ScienceDirect

Journal of Taibah University for Science 10 (2016) 168–180

Journal of Taibah University for Science

www.elsevier.com/locate/jtusci

Synthesis of bisimidazolium–ionic liquids: Characterization, thermal stability and application to bentonite intercalation

Benamar Makhoukhi [a,*], Didier Villemin [b], Mohamed Amine Didi [a]

[a] *Laboratory of Separation and Purification Technologies, Department of Chemistry, Tlemcen University, Box 119, Tlemcen, Algeria*
[b] *Laboratoire de Chimie Moléculaire et Thio-organique, UMR CNRS 6507, INC3M, FR 3038, ENSICAEN & Université de Caen, 14050 Caen, France*

Received 2 April 2015; received in revised form 15 August 2015; accepted 21 August 2015
Available online 10 November 2015

Abstract

In this study, a convenient method was developed for the synthesis of bisimidazolium salts and bisimidazolium–ionic liquids. The products were characterized by nuclear magnetic resonance (NMR), Fourier transform infrared spectroscopy (FTIR), mass spectroscopy, elemental analysis and thermogravimetric analyses (TGA). The effect of the counter ion, alkyl chain length and structural isomerism on the thermal stability of the bisimidazolium salts was investigated. Ionic liquid-treated bentonite clays were prepared by ion exchange of the bisimidazolium cations with Na-bentonite. These new organoclays were characterized by X-ray diffraction (XRD), FTIR and TGA. The results show that the ionic liquid-intercalated bentonites have greater thermal stability (450–470 °C) compared with the bisimidazolium- or the diphosphonium-exchanged bentonites.

Keywords: Ionic liquids; Bisimidazolium salts; Thermal stability; Bentonite; Organoclay

1. Introduction

In recent years, the use of imidazolium salts in environmentally benign chemical processes and chemical analyses has dramatically increased [1]. Imidazolium salts are important in organic synthesis, such as in the synthesis of new achiral and chiral ionic liquids [2], complexed with metals as good to excellent catalysts in the Heck reaction [3], and complexed with Pd (II) as active catalysts for the Heck and Suzuki-Miyaura cross-coupling reactions [4]. In addition, bisimadozolium salts are used as levelling agents in the dyeing of acrylic fibres [5] and as softening agents for cotton and cotton-polyester blends [6].

Recently, ionic liquids (ILs) have received much attention because of their unique characteristics, such as low volatility, non-flammability, high thermal stability, high ionic conductivity and stability up to a temperature of 400 °C [7]. Typically, ionic liquids are substances with melting points below 100 °C and consist of a bulky, asymmetric organic cation (e.g., imidazolium,

* Corresponding author. Tel.: +213 43213198; fax: +213 43213198.
E-mail address: benamarmakh@yahoo.fr (B. Makhoukhi).
Peer review under responsibility of Taibah University.

Production and hosting by Elsevier

http://dx.doi.org/10.1016/j.jtusci.2015.08.005

pyridinium, alkylphosphonium or alkylammonium ions) and a smaller inorganic anion.

Ionic liquids based on imidazolium cations have been extensively studied as non-volatile electrolytes in nc-TiO_2-based dye-sensitized solar cells due to their good stability and high ionic conductivity [8]. Imidazolium–ILs, such as (1-butyl-3-methylimidazolium bis(trifluoromethane sulfonyl)imide [Bmim][$N(Tf)_2$]), have been used in organic light-emitting devices [9]. It has been reported that using these ionic liquids in thin film transistors as an electrolyte component improves the device characteristics [10]. Investigations into the use of imidazolium-based ILs for capacitors, fuel cells and batteries have been performed [11].

Currently, the applications of ionic liquids in polymer material processing have received attention [12,13]. These salts have been used to improve the thermal stability of functionalized material because the thermal stability of the imidazolium cation can be improved based on the substituent at various positions on the imidazole ring, the counter ion, the alkyl chain length, and the isomeric structure of the alkyl side group [13,14].

A recent study reported the synthesis of a promising organoclay that exhibited substantially higher thermal stability than ammonium or phosphonium cation-modified organoclays [13–15]. The success of high-performance nanocomposites depends on the stability of the organic modifier used in the functionalization of clay, as the organic treatment is the interface between the layered silicate and the polymer [11]. A poor interface between polymer and layered silicate will often result in a microcomposite or in a traditional filled system.

The present study describes the synthesis and characterization of new bisimidazolium dichlorides and bisimidazolium–ILs with higher thermal stability. The synthesis of bisimidazolium was based on the reaction of bis(chloromethyl)benzenes with imidazoles. For the preparation of ionic liquids, bis(trifluoromethane)sulfonimide lithium ($LiNTf_2$) and ammonium hexafluorophosphate (PF_6) were used. Finally, sodium bentonite (Na–Bt) was intercalated with [ILs-NTf_2] and [ILs-PF_6] to prepare the new organoclays with higher thermal stability.

2. Experimental

2.1. Synthesis and characterization of bis-imidazolium salts

A general procedure for the synthesis of various bis-imidazolium dichlorides consists of refluxing bis(chloromethyl) benzene with imidazoles in dimethylformamide (DMF) with a molar ratio of 1:2. Under the classical conditions, the mixtures were heated and stirred at 120 °C for 6 h (Fig. 1).

2.1.1. 3,3′-(1,4-phenylenebis(methylene))bis(1-methyl-1H-imidazol-3-ium) dichloride [p.MeBIM]

A mixture of 1,4-bis(chloromethyl) benzene (1.748 g; 10 mmol) and 1-methyl imidazole (1.64 g; 20 mmol) in dimethylformamide (DMF) was heated and stirred at 120 °C for 6 h.

A precipitate of salt was formed while the mixture was hot. After cooling (20 °C), the solution was filtered under vacuum, and the solid was washed with the dry diethyl ether (50 mL). The solid white precipitate was dried under vacuum at 20 °C for 1 h. Yield (89%).

^{1}H NMR (D_2O) δ_H (ppm): 3.68(CH_3, 6H, d), 5.22(CH_2, 4H, d), 7.25(4H, m), 7.49(2H, t), 7.56 (2H, t), 9.06 (2H, s). ^{13}C NMR (D_2O) δ_C (ppm): 2C(35.69), 2C(52.25), 4C_{imd}(122.21), 2C_{arm}(123.80), 4C_{arm}(129.23), 2C_{imd}(134.58).

FT-IR ν (cm^{-1}): 731–856(C–H), 1161(C–N), 1333(CH_3), 1450(C=$_{arm}$), 1562(C=N).

$C_{16}H_{20}N_4Cl_2$: Calcd. (%C 56.6, %H 5.9, %N 16.5) Observed (%C 56.4, %H 5.8, %N 16.7). HRMS (ESI+) *m/z* calcd. for $[C_{16}H_{20}N_4Cl_1]^+$: 302.65; found 302.66.

2.1.2. 3,3′-(1,3-phenylenebis(methylene))bis(1-methyl-1H-imidazol-3-ium) dichloride [m.MeBIM]

A mixture of 1,3-bis(chloromethyl) benzene (1.748 g; 10 mmol) and 1-methyl imidazole (1.64 g; 20 mmol) in DMF was heated and stirred at 120 °C for 6 h. The solid yellow precipitate was dried under vacuum at 20 °C for 1 h. Yield (70%).

^{1}H NMR (D_2O) δ_H: 3.87(CH_3, 6H, d), 5.40(CH_2, 4H, d), 7.48(4H, m), 7.69(2H, t), 8.57(2H, s), 9.16(2H, s). ^{13}C NMR (D_2O) δ_C: 2C(35.66), 2C(52.34), 4C_{imd}(122.12), 4C_{arm}(127.67), 2C_{imd}(129.15), 2C_{arm}(133.18). FT-IR ν (cm^{-1}): 752–803(C–H), 1159(C–N), 1359(CH_3), 1451(C=$_{arm}$), 1573(C–C), 1634(C=N).

$C_{16}H_{20}N_4Cl_2$: Calcd. (%C 56.6, %H 5.9, %N 16.5) Observed (%C 56.5, %H 5.9, %N 16.8). HRMS (ESI+) *m/z* calcd. for $[C_{16}H_{20}N_4Cl_1]^+$: 302.65; found 302.66.

2.1.3. 3,3′-(1,2-phenylenebis(methylene))bis(1-methyl-1H-imidazol-3-ium) dichloride [o.MeBIM]

A mixture of 1,2-bis-(chloromethyl) benzene (1.748 g; 10 mmol) and 1-methyl imidazole (1.64 g;

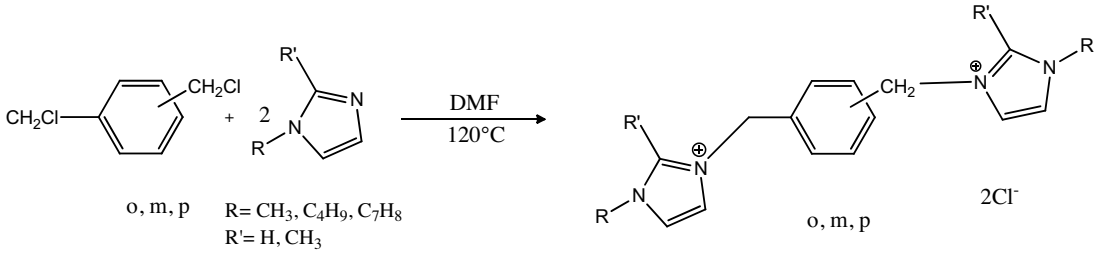

Fig. 1. Synthesis of bis-imidazolium dichloride. R = CH_3, R′ = H: (o, m, p) MeBIM; R = CH_3, R′ = CH_3: (o, m, p) DMeBIM; R = C_4H_9, R′ = H: (o, m, p) BuBIM; R = C_7H_8, R′ = H: (o, m, p) BzBIM.

20 mmol) in DMF was heated and stirred at 120 °C for 6 h. The solid white precipitate was dried under vacuum at 20 °C for 1 h. Yield (95%).

^{1}H NMR (D_2O) δ_H: 3.82(CH_3, 6H, d), 5.47(CH_2, 4H, d), 7.40(4H, m), 7.45(2H, t), 7.57(2H, m), 8.95(2H, s). ^{13}C NMR (D_2O) δ_C: 2C(35.66), 2C(52.36), $4C_{imd}$(123.77), $2C_{arm}$(127.50), $2C_{arm}$(129.15), $2C_{imd}$(133.18), $2C_{arm}$(140.43). FT-IR ν (cm^{-1}): 765–882(C–H), 1173(C–N), 1359(CH_3), 1424($C=_{arm}$), 1580(C–C), 1644(C=N).

$C_{16}H_{20}N_4Cl_2$: Calcd. (%C 56.6, %H 5.9, %N 16.5) Observed (%C 56.3, %H 6.0, %N 16.7). HRMS (ESI+) *m/z* calcd. for $[C_{16}H_{20}N_4Cl_1]^+$: 302.65; found 302.66.

*2.1.4. 3,3′-(1,4-phenylenebis(methylene))bis(1,2-dimethyl-1*H*-imidazol-3-ium) dichloride [p.DMeBIM]*

A mixture of 1,2-bis-(chloromethyl) benzene (1.748 g; 10 mmol) and 1,2-bis(methyl) imidazole (1.64 g; 20 mmol) in DMF (40 mL) was heated and stirred at 120 °C for 6 h. A precipitate of salt was formed while the mixture was hot. After cooling (20 °C), the solution was filtered under vacuum, and the solid was washed with the dry diethyl ether (100 mL). The solid white precipitate was dried under vacuum at 20 °C for 1 h. Yield (90%).

^{1}H NMR (D_2O) δ_H: 2.53(CH_3, 6H, d), 3.75(CH_3, 6H, d), 5.36(CH_2, 4H, d), 7.32(4H, m), 7.82(2H, t), 8.86(2H, s). ^{13}C NMR (D_2O) δ_C: 2C(9.03), 2C(34.06), 2C(50.93), $2C_{imd}$(121.10), $2C_{imd}$(122.43), $4C_{arm}$(128.32), $2C_{arm}$(134.33), $2C_{imd}$(144.74).

FT-IR ν (cm^{-1}): 740–809(C–H), 1177(C–N), 1370(CH_3), 1456($C=_{arm}$), 1589(C–C), 1701(C=N). $C_{18}H_{24}N_4Cl_2$: Calcd. (%C 58.9, %H 6.6, %N 15.2) Observed (%C 58.7, %H 6.9, %N 15.4). HRMS (ESI+) *m/z* calcd. for $[C_{18}H_{24}N_4Cl_1]^+$: 330.68; found 330.69.

*2.1.5. 3,3′-(1,3-phenylenebis(methylene))bis(1,2-dimethyl-1*H*-imidazol-3-ium) dichloride [m.DMeBIM]*

A mixture of 1,3-bis(chloromethyl) benzene (1.748 g; 10 mmol) and 1,2-bis(methyl) imidazole (1.64 g; 20 mmol) in DMF (40 mL) was heated and stirred at 120 °C for 6 h. The solid white precipitate was dried under vacuum at 20 °C for 1 h. Yield (70%).

^{1}H NMR (D_2O) δ_H: 2.50(CH_3, 6H, d), 3.73(CH_3, 6H, d), 5.35(CH_2, 4H, d), 6.84(3H, m) 7.33(1H, d), 7.46(2H, m), 8.25(2H, s). ^{13}C NMR (D_2O) δ_C: 2C(9.16), 2C(32.76), 2C(51.07), $4C_{imd}$(121.84), $1C_{arm}$(126.90), $2C_{arm}$(127.90), $1C_{arm}$(130.14), $2C_{arm}$(134.79), $2C_{imd}$(144.78). FT-IR ν (cm^{-1}): 751–810(C–H), 1170(C–N), 1376(CH_3), 1510($C=_{arm}$), 1607(C–C), 1707(C=N).

$C_{18}H_{24}N_4Cl_2$: Calcd. (%C 58.9, %H 6.6, %N 15.2) Observed (%C 58.6, %H 6.8, %N 15.4). HRMS (ESI+) *m/z* calcd. for $[C_{18}H_{24}N_4Cl_1]^+$: 330.68; found 330.69.

*2.1.6. 3,3′-(1,2-phenylenebis(methylene))bis(1,2-dimethyl-1*H*-imidazol-3-ium) dichloride [o.DMeBIM]*

A mixture of 1,2-bis(chloromethyl) benzene (1.748 g; 10 mmol) and 1,2-bis(methyl) imidazole (1.64 g; 20 mmol) in DMF (40 mL) was heated and stirred at 120 °C for 6 h. The solid white precipitate was dried under vacuum at 20 °C for 1 h. Yield (87%).

^{1}H NMR (D_2O) δ_H: 2.54(CH_3, 6H, d), 3.80(CH_3, 6H, d), 5.41(CH_2, 4H, d), 7.03(2H, m) 7.2(2H, d), 7.45(2H, m), 8.14(2H, s). ^{13}C NMR (D_2O) δ_C: 2C(9.02), 2C(34.78), 2C(48.64), $2C_{imd}$(120.93), $2C_{imd}$(122.65), $2C_{arm}$(128.44), $2C_{arm}$(129.79), $2C_{arm}$(131.08), $2C_{imd}$(145.12). FT-IR ν (cm^{-1}): 709–880(C–H), 1160(C–N), 1337(CH_3), 1455($C=_{arm}$), 1560(C–C), 1639(C=N).

$C_{18}H_{24}N_4Cl_2$: Calcd. (%C 58.9, %H 6.6, %N 15.2) Observed (%C 58.7, %H 6.5, %N 15.3). HRMS (ESI+) *m/z* calcd. for $[C_{18}H_{24}N_4Cl_1]^+$: 330.68; found 330.69.

*2.1.7. 3,3′-(1,4-phenylenebis(methylene))bis(1-butyl-1*H*-imidazol-3-ium) dichloride [p.BuBIM]*

A mixture of 1,4-bis(chloromethyl) benzene (1.748 g; 10 mmol) and 1-butyl imidazole (2.48 g; 20 mmol) in DMF (40 mL) was heated and stirred at 120 °C for 8 h. A precipitate of salt was formed while the mixture was hot. After cooling (20 °C), the solution was filtered under vacuum, and the solid was washed with dry diethyl ether (100 mL). The solid white precipitate was dried under vacuum at 20 °C for 1 h. Yield (78%).

^{1}H NMR (D_2O) δ_H: 0.90(CH_3, 6H, m), 1.28(CH_2, 4H, m), 1.84(CH_2, 4H, m), 4.20(CH_2, 4H, m), 5.40(CH_2, 4H, d), 7.46(4H, m), 7.75(2H, d), 8.83(2H, m), 9.20(2H, s).

^{13}C NMR (D_2O) δ_C: 2C(12.56), 2C(18.70), 2C(31.14), 2C(49.46), 2C(52.32), $4C_{imd}$(122), $4C_{arm}$(129.23), $2C_{arm}$(134.70), $2C_{imd}$(135.39).

FT-IR ν (cm^{-1}): 723–863(C–H), 1160(C–N), 1359(CH_3), 1442($C=_{arm}$), 1561(C–C), 1646(C=N). $C_{22}H_{32}N_4Cl_2$: Calcd. (%C 62.4, %H 7.6, %N 13.2) Observed (%C 62.2, %H 7.8, %N 13.4). HRMS (ESI+) *m/z* calcd. for $[C_{22}H_{32}N_4Cl_1]^+$: 386.74; found 386.75.

*2.1.8. 3,3′-(1,3-phenylenebis(methylene))bis(1-butyl-1*H*-imidazol-3-ium) dichloride [m.BuBIM]*

A mixture of 1,3-bis(chloromethyl) benzene (1.748 g; 10 mmol) and 1-butyl imidazole (2.48 g; 20 mmol) in DMF (40 mL) was heated and stirred at 120 °C for 8 h. A viscous liquid was formed while the mixture was hot, and the solvent (DMF) was evaporated. Yield (75%).

^{1}H NMR (D_2O) δ_H: 0.86(CH_3, 6H, m), 1.29(CH_2, 4H, m), 1.80(CH_2, 4H, m), 4.14(CH_2, 4H, m), 5.39(CH_2, 4H, m), 7.54(4H, m), 7.91(2H, d), 8.82(2H, m), 9.22(2H, s).

^{13}C NMR (D_2O) δ_C: 2C(12.56), 2C(18.88), 2C(31.13), 2C(49.43), 2C(52.38), $4C_{imd}$(122.33), $2C_{arm}$(128.22), $2C_{arm}$(129.17), $2C_{arm}$(130.27), $2C_{imd}$(134.78).

FT-IR ν (cm^{-1}): 733–820(C–H), 1154(C–N), 1361(CH_3), 1511($C=_{arm}$), 1559(C–C), 1633(C=N). $C_{22}H_{32}N_4Cl_2$: Calcd. (%C 62.4, %H 7.6, %N 13.2) Observed (%C 62.1, %H 7.7, %N 13.5). HRMS (ESI+) *m/z* calcd. for $[C_{22}H_{32}N_4Cl_1]^+$: 386.74; found 386.75.

2.1.9. 3,3′-(1,2-phenylenebis(methylene))bis(1-butyl-1H-imidazol-3-ium) dichloride [o.BuBIM]

A mixture of 1,2-bis(chloromethyl) benzene (1.748 g; 10 mmol) and 1-butyl imidazole (2.48 g; 20 mmol) in DMF (40 mL) was heated and stirred at 120 °C for 8 h. The solid white precipitate was dried under vacuum at 20 °C for 1 h. Yield (73%).

^{1}H NMR (D_2O) δ_H: 0.93(CH_3, 6H, m), 1.25(CH_2, 4H, m), 1.82(CH_2, 4H, m), 4.19(CH_2, 4H, m), 5.51(CH_2, 4H, m), 7.35(4H, m), 7.61(2H, d), 8.70(2H, m), 9.11(2H, s).

^{13}C NMR (D_2O) δ_C: 2C(12.57), 2C(18.75), 2C(31.24), 2C(49.57), 2C(49.98), $4C_{imd}$(122), $4C_{arm}$(131.12), 4C(135.38). FT-IR ν (cm^{-1}): 744(C–H), 1170(C–N), 1294(CH_3), 1538($C=_{arm}$), 1590(C–C), 1640(C=N).

$C_{22}H_{32}N_4Cl_2$: Calcd. (%C 62.4, %H 7.6, %N 13.2) Observed (%C 62.3, %H 7.7, %N 13.3). HRMS (ESI+) *m/z* calcd. for $[C_{22}H_{32}N_4Cl_1]^+$: 386.74; found 386.75.

*2.1.10. 3,3′-(1,4-phenylenebis(methylene))bis(1-benzyl-1*H*-imidazol-3-ium) dichloride [p.BzBIM]*

A mixture of 1,4-bis(chloromethyl) benzene (0.44 g; 2.5 mmol) and 1-benzyl imidazole (0.79 g; 5 mmol) in DMF (40 mL) was heated and stirred at 140 °C for 8 h. A precipitate of salt was formed while the mixture was hot. After cooling (20 °C), the solution was filtered under vacuum, and the solid was washed with dry diethyl ether (100 mL) and acetone (40 mL). The solid white precipitate was dried under vacuum at 20 °C for 1 h. Yield (65%).

^{1}H NMR (D_2O) δ_H: 5.4(CH_2, 4H, d), 5.65(CH_2, 4H, m), 7.42(4H, m), 7.65(12H, m), 8.88(2H, d), 9.24(2H, s). ^{13}C NMR (D_2O) δ_C: 2C(52.46), 2C(53.64), $4C_{imd}$(122.92), $6C_{arm}$(128.67), $6C_{arm}$(129.57), $2C_{arm}$(133.42), $1C_{imd}$(134.56), $1C_{imd}$(135.60).

FT-IR ν (cm^{-1}): 709–897(C–H), 1145(C–N), 1320(CH_2), 1454($C=_{arm}$), 1559(C=N).

$C_{28}H_{28}N_4Cl_2$: Calcd. (%C 68.4, %H 5.7, %N 11.4) Observed (%C 68.1, %H 5.9, %N 11.6). HRMS (ESI+) *m/z* calcd. for $[C_{28}H_{28}N_4Cl_1]^+$: 454.71; found 454.72.

*2.1.11. 3,3′-(1,3-phenylenebis(methylene))bis(1-benzyl-1*H*-imidazol-3-ium) dichloride [m.BzBIM]*

A mixture of 1,3-bis(chloromethyl) benzene (0.44 g; 2.5 mmol) and 1-benzyl imidazole (0.79 g; 5 mmol) in DMF (40 mL) was heated and stirred at 140 °C for 8 h. A precipitate of salt was formed while the mixture was

hot. The solid white precipitate was dried for 1 h under vacuum at 20 °C. Yield (60%).

^{1}H NMR (D_2O) δ_H: 2.83(CH_2, 2H, m), 2.98(CH_2, 2H, s), 5.36(CH_2, 4H, m), 7.43(4H, m), 7.69(12H, m), 8.89(2H, m), 9.18(2H, s). ^{13}C NMR (D_2O) δ_C: 4C(52.62), 4C_{imd}(122.92), 6C_{arm}(128.47), 6C_{arm}(129.85), 2C_{arm}(133.91), 1C_{imd}(135.26), 1C_{imd}(136.12). FT-IR ν (cm^{-1}): 710–879(C–H), 1148(C–N), 1454(C=$_{arm}$), 1557(C–C), 1661 (C=N). $C_{28}H_{28}N_4Cl_2$: Calcd. (%C 68.4, %H 5.7, %N 11.4) Observed (%C 68.2, %H 5.8, %N 11.5). HRMS (ESI+) *m/z* calcd. for $[C_{28}H_{28}N_4Cl_1]^+$: 454.71; found 454.72.

*2.1.12. 3,3′-(1,2-phenylenebis(methylene))bis(1-benzyl-1*H*-imidazol-3-ium) dichloride [o.BzBIM]*

A mixture of 1,3-bis(chloromethyl) benzene (0.44 g; 2.5 mmol) and 1-benzyl imidazole (0.79 g; 5 mmol) in DMF (40 mL) was heated and stirred at 140 °C for 8 h. A precipitate of salt was formed while the mixture was hot. The solid white precipitate was dried (1 h) under vacuum at 20 °C. Yield (55%).

^{1}H NMR (D_2O) δ_H: 2.25(CH_2, 2H, s), 2.87(CH_2, 2H, s), 5.52(CH_2, 4H, d), 7.59(4H, m), 8.48(12H, m), 8.89(2H, m), 9.15(2H, s). ^{13}C NMR (D_2O) δ_C: 2C(50.86), 2C(53.21), 4C_{imd}(122.0), 6C_{arm}(128.92), 6C_{arm}(129.88), 2C_{arm}(131.30), 1C_{imd}(132.39), 1C_{imd}(133.18). FT-IR ν (cm^{-1}): 709–891(C–H), 1148(C–N), 1387(CH_2), 1454(C=$_{arm}$), 1557(C–C), 1662(C=N). $C_{28}H_{28}N_4Cl_2$: Calcd. (%C 68.4, %H 5.7, %N 11.4) Observed (%C 68.3, %H 5.8, %N 11.5). HRMS (ESI+) *m/z* calcd. for $[C_{28}H_{28}N_4Cl_1]^+$: 454.71; found 454.72.

2.2. Synthesis of bisimidazolium–ionic liquids

The use of 3,3′-(1,4-phenylenebis(methylene))bis(1-methyl-1*H*-imidazol-3-ium) dichloride [p.MeBIM] permits the synthesis of substituted ionic liquids, such as bis(trifluoromethane)sulfonimide lithium ($LiNTf_2$), by heating and microwave irradiation with the addition of ammonium hexafluorophosphate (PF_6).

*2.2.1. 3,3′-(1,4-phenylenebis(methylene))bis(1-methyl-1*H*-imidazol-3-ium)bis(trifluoromethane sulfonyl)imide [MeBIM-NTf$_2$]*

Bis-imidazolium dichloride [p.MeBIM] (0.339 g, 1 mmol) was added to water (20 mL) in a flask and was heated to 70 °C. The mixture was stirred for approximately 30 min at this temperature. Bis(trifluoromethane)sulfonimide lithium [$LiN(SO_2CF_3)_2$] (0.574 g, 2 mmol) was also dissolved in water (20 mL) and was added to the stirring solution of bisimidazolium salt. The colour of the transparent solution turned cloudy white. The mixture was stirred for approximately 24 h at room temperature to allow the ion exchange reaction to proceed, to yield a yellowish, sticky compound. Acetone was added to the mixture, and bisimidazolium-IL was extracted from the water. Then, the solvent was evaporated, and a yellowish gel-like compound was obtained. This gel-like compound was allowed to stand at room temperature, and a yellowish quasi-solid compound was obtained after two weeks by evaporation of the acetone solvent. Yield (95%).

^{1}H NMR (CD_3COCD_3) δ_H (ppm): 3.71(CH_3, 6H, d), 5.11(CH_2, 4H, d), 7.08(2H, t), 7.19(4H, m), 7.56(2H, t), 8.06(2H, s). ^{19}F NMR (CD_3COCD_3) δ_F(ppm): 97.54; for ($LiN(CF_3SO_2)_2$): ^{19}F NMR δ_F(ppm): −79.23. FTIR ν (cm^{-1}): 3150–3200(C–H_{arm}), 1630(C=N), 1510(C=$_{arm}$), 1540(C–C), 1200(S–O). $C_{20}H_{20}F_{12}N_6O_8S_4$: Calcd. (%C 28.99, %H 2.43, %N 10.14) Observed (%C 28.80, %H 2.28, %N 10.17).

*2.2.2. 3,3′-(1,4-phenylenebis(methylene)) bis(1-methyl-1*H*-imidazol-3-ium)bis (hexafluorophosphate) [MeBIM-PF$_6$]*

A mixture of [p.MeBIM] (0.848 g, 2.5 mmol) dissolved in 10 mL of distilled water and bis(ammoniumhexafluorophosphate) (0.815 g, 5 mmol) dissolved in 10 mL of distilled water were combined. The mixture was irradiated to 20 W for 5 min, the tempetarure reached 140 °C, and a release of ammonia gas was observed. A viscous liquid (yellow) was formed, and after cooling at room temperature, several washings with acetone (100 mL) yielded a white precipitate that was filtered. Yield (93%).

^{1}H NMR (D_2O) δ_H (ppm): 3.66(CH_3, 6H, d), 4.90(CH_2, 4H, d), 7.06(4H, t), 7.12(4H, m), 7.76(2H, s). ^{19}F NMR (D_2O) δ_F (ppm): 103.62; for (NH_4PF_6): ^{19}F NMR (D_2O) δ_F (ppm): −73.60. ^{31}P NMR (D_2O) δ_F (ppm): −144.16; for (NH_4PF_6): ^{31}P NMR (D_2O) δ_F(ppm): −145.11. FTIR ν (cm^{-1}): 3150(C–H_{ar}), 1560(C=N), 1450(C=$_{ar}$), 1340(CH_3), 1160(N–P). $C_{16}H_{20}F_{12}N_4P_2$: Calcd. (%C 34.42, %H 3.61, %N 10.04) Observed (%C 34.24, %H 3.55, %N 10.12).

2.3. Bentonite sample

The natural bentonite used in this study was obtained from deposits in the area of Maghnia, Algeria. The chemical composition of bentonite, as determined by X-ray fluorescence (Philips PW 3710), was found to be as

follows: 62.48% SiO_2, 17.53% Al_2O_3, 1.23% Fe_2O_3, 3.59% MgO, 0.82% K_2O, 0.87% CaO, 0.22% TiO_2, 0.39% Na_2O, 0.04% As, and 13.0% loss on ignition at 950 °C [16,17]. The mineralogical analysis showed that the native crude clay mineral predominantly contains montmorillonite (86 wt.%). The clay composition also contains quartz (10%), cristoballite (3.0%) and beidellite (less than 1%) [18,19].

To purify bentonite, 120 g of natural bentonite was dispersed in 1.5 L of distilled water, and after agitation for 15 min, a buffer solution of sodium citrate (pH = 7.3) was added. The mixture was heated under agitation at 75 °C for 20 min, and then, 15 g of sodium thiosulfate ($Na_2S_2O_4$) was slowly added. After 15 min under agitation, the mixture was cooled and centrifuged at a rotational speed of 6000 rpm (centrifugal type JA 10) for 15 min. The recovered solid was washed two times with 0.05 M HCl (1.5 L) for 3 h.

The purified bentonite was converted into sodium bentonite as follows: an amount of bentonite was dispersed in a 1 M NaCl solution with a 1/5 mass ratio. After agitation for 2 h, the solid was separated by centrifugation at a rotational speed of 6000 rpm for 15 min; this operation was repeated three times. The solid was washed three times with distilled water and was dried at 40 °C for three days.

The chemical composition of purified bentonite was found to be as follows: 64.7% SiO_2, 18.1% Al_2O_3, 0.95% Fe_2O_3, 2.66% MgO, 0.8% K_2O, 0.61% CaO, 0.2% TiO_2, 1.43% Na_2O, 0.05% As, and 10.0% loss on ignition [16–19].

The cation-exchange capacity (CEC) of bentonites was determined according to the ammonium acetate saturation method and was found to be 70 meq per 100 g of dry natural-Bt and 98 meq per 100 g of dry Na-Bt. The BET specific surface area increased from 50 m^2/g in natural-Bt to 95 m^2/g in Na-Bt.

2.4. Preparation of organo-clays

The intercalation of the bisimidazolium–ILs into the Na–bentonite channels was performed by a cationic exchange reaction following a previously described procedure [13] in which 10 g of Na-bentonite was dispersed into 200 mL of hot water under continuous stirring for approximately 4 h.

A predissolved stoichiometric amount of bisimidazolium–ILs solution (3.0 CEC of the bentonite) was slowly added to the bentonite suspension under strong stirring at room temperature (20 ± 2 °C). The concentration of bisimidazolium–ILs used in this study is 3.0 CEC of the bentonite (the concentrations of 1.0 and 2.0 CEC of the bentonite were also tested to evaluate the effect of surfactant concentration on the interlayer structure of the organoclay).

The reaction mixtures were stirred for 20 h at room temperature (20 ± 2 °C). All of the organoclay products were then centrifuged at 3000 rpm for 10 min, washed several times with distilled water, dried in a convection oven at 80 °C for 24 h and, finally, crushed in a mortar. The sieved organic bentonites with a size less than 53 μm were used for characterization.

The chemical composition of intercalated bentonite ([p.MeBIM–PF_6]–Bt) was found to be as follows: 66.87% SiO_2, 18.64% Al_2O_3, 1.83% Fe_2O_3, 2.12% MgO, 0.56% K_2O, 0.25% CaO, 0.2% TiO_2, 0.31% Na_2O, 0.05% As, and 9.15% loss on ignition.

The chemical composition of the second organoclay ([p.MeBIM–NTf_2]–Bt) was found to be as follows: 67.23% SiO_2, 18.36% Al_2O_3, 1.68% Fe_2O_3, 1.75% MgO, 0.42% K_2O, 0.28% CaO, 0.2% TiO_2, 0.23% Na_2O, 0.05% As, and 9.8% loss on ignition.

2.5. Characterization techniques

FTIR spectra were obtained with solids or neat liquids using a Perkin Elmer 16 PC Fourier transform infrared spectrometer with an ATR accessory. The ^1H, ^{13}C, ^{19}F and ^{31}P NMR spectra were recorded in D_2O using a Fourier Bruker AC 400 multinuclear spectrometer. Mass spectra were recorded on a QTOF Micro (Waters) spectrometer with electrospray ionization (ESI, positive mode), lockspray PEG, infusion introduction at 5 mL/min, a source temperature of 80 °C and a desolvation temperature of 120 °C. Elemental analyses were recorded using an automatic apparatus CHNS-O ThermoQuest. The XRD patterns of intercalated bentonites were collected on a Philips X-Pert diffractometer using Ni filtered Cu-Ka radiation. The thermogravimetric analyses (TGA) of the samples were performed using a Perkin Elmer TGA-7 thermogravimetric analyser.

3. Results and discussion

3.1. TGA of bisimidazolium cations and bisimidazolium–ILs

Thermogravimetric measurements were carried out on a series of bisimidazolium salts. Although the bisimidazolium salts considered here have the same anion (Cl), their structures differ in terms of cation structures. The T_{onset} values for the products range from 350 to 480 °C, as presented in Fig. 2. The results are reported in terms of

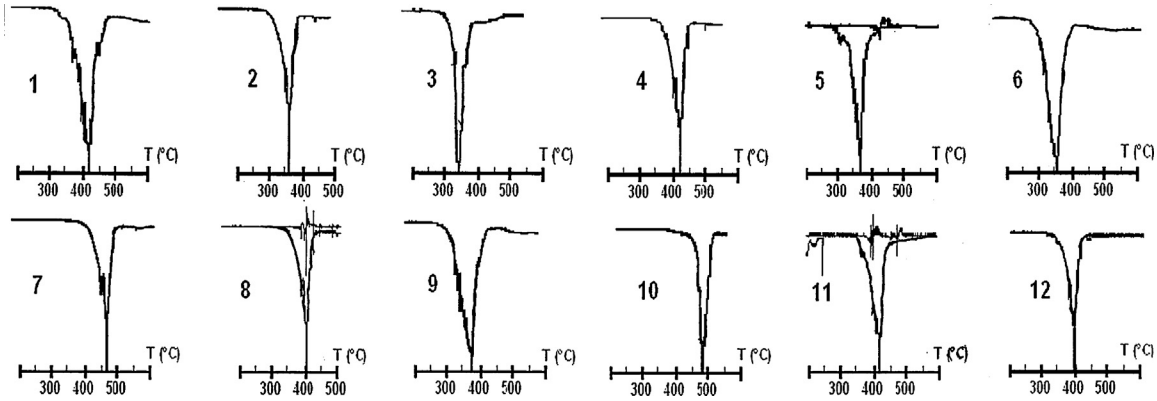

Fig. 2. DTG curves of bisimidazolium salts. (1) p.MeBIM, (2) m.MeBIM, (3) o.MeBIM; (4) p.DMeBIM, (5) m.DMeBIM, (6) o.DMeBIM; (7) p.BuBIM, (8) m.BuBIM, (9) o.BuBIM; (10) p.BzBIM, (11) m.BzBIM, (12) o.BzBIM.

the onset decomposition temperature (5% mass fraction loss) and the peak decomposition temperature, both of which have an uncertainty of ±3 °C. The onset temperature values (T_{onset}) reported here were obtained from the interception of two linear functions, one originating from the zero weight loss level and the other one being tangent to the decreasing portion of the weight change line. Because T_{onset} typically overestimates the thermal decomposition temperature, especially at this relatively high heating rate, all of our analyses were based on the T'_{onset} values obtained from the onsets of derivative weight % change lines.

Important observations can be drawn from results:

- TGA shows that the thermal decomposition of products occurred in one step, and the maximum decomposition rate was different for all of the substances. In contrast, the derivative TGA indicated that the thermal decomposition of the bisimidazolium salts occurred in two steps. The mass-loss of water desorption was observed at 100–200 °C and accounted for up to 2–5% of the original mass. A very large amount of mass-loss (<90%) was shown over the temperature range of 300–450 °C, which is related to the thermal decomposition of the product. Thus, the bisimidazolium salts exhibited good thermal stability, considering normal polymer processing temperatures in the range of 300–450 °C.
- The imidazolium cation is more thermally stable than the alkyl ammonium or the alkyl phosphonium cation. This observation has been reported in previously studies [13,15], which indicated that the imidazole is resistant to ring fission during thermal rearrangements of 1-alkyl- and 1-aryl imidazoles at temperatures above 600 °C.
- The bisimidazolium thermal stability is affected by the type of isomeric structure of the alkyl side group. Fig. 2 shows that the onset temperature of decomposition for benzylbisimidazolium, it is close to 400–480 °C, for butylbisimidazolium, it is close to 380–460 °C, for dimethylbisimidazolium, it is close to 360–420 °C and for methylbisimidazolium, it is close to 350–420 °C. In addition, a relationship was observed between the chain length of the alkyl group attached to the nitrogen atom and the oxidative decomposition of the bisimidazolium salts, indicating that the thermal stability increases as the organic content of the molecule increases. This is evidenced by the observation that the thermal stability increases in the following order: bis(benzyl-imidazolium), bis(butyl-imidazolium), bis(dimethyl-imidazolium), bis(methyl-imidazolium). On the other hand, it was noticed that the presence of oxygen does not appear to have any effect on the breakdown of the halide salts. This may reflect that the activation energy required for the thermal decomposition of the halide salts is lower than that for their oxidative decomposition [20].
- The thermal stability of para(bisimidazolium) was higher than that observed with meta and ortho (bisimidazolium). The geometric effects of the molecules play an important role, and it is clearly seen that the thermal stability of the para compounds is better than meta, which is better than ortho. For example, in the case of p.MeBIM, the onset temperatures of decomposition are close to 420 °C, for m. MeBIM, they are close to 360 °C and for o.MeBIM, they are close to 350 °C. The onset temperature of the decomposition for p.BuBIM is close to 460 °C, for m.BuBIM, close to 400 °C and for o.BuBIM, close to 380 °C. The same remark was observed in the case of (p, m, o) DMeBIM and in the case of (p, m, o) BzBIM

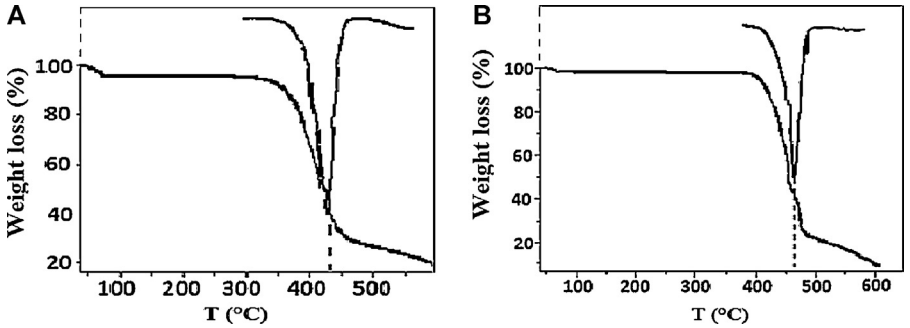

Fig. 3. TGA (DTG) curves of bisimidazolium–ILs. (A) [p.MeBIM–NTf_2]; (B) [p.MeBIM–PF_6].

(Fig. 2) in which the weight-loss of para products was larger than that of meta and ortho products.

- Methyl substitution in the 2-position enhances the thermal stability. This is evident from the increase in the onset decomposition temperature of bis(dimethylimidazolium) salts compared with bis(methylimidazolium) salts. This may be due to the high acidic characteristics of the C-2 proton [20]. The most acidic proton on the imidazolium cation is the proton located at the C-2 position, which is the carbon atom between the two N atoms of the imidazolium ring [21]. This proton is responsible for the strongly localized and directional hydrogen bond between cation and anion. Thus, it contributes to the inter-ionic cohesive energy, which decreases with increasing acidity of this proton, i.e., with increasing C2–H bond strength [21]. The acidity of this proton was quantified by the stretching vibration frequency of the C2–H bond, ν (C2–H). Because all of the bisimidazolium salts considered in this study have the same cation, any change in the anion structure results in a change in the inter-ionic interaction strength and the acidity of C2–H. In general, a higher ν (C2–H) value represents a higher energy of the C2–H bond, thus indicating a higher C2–H acidity [22].

Concerning the thermogravimetric analysis of bisimidazolium–ionic liquids, Fig. 3 shows the TGA curves for [p.MeBIM–ILs] and the corresponding derivative weight loss curves. Although the ILs considered in this study have the same cation, their structures differ in terms of the anion. The T_{onset} values for the ILs range from 420 to 460 °C, as given in Fig. 3. Thus, we infer that the anion structure has a significant effect on the thermal stability limits, as discussed in various studies [23,24].

For the bisimidazolium dichloride used in [p.MeBIM], the onset temperature is close to 420 °C. For the prepared ionic liquids, the onset temperature of decomposition for [ILs.NTf_2] is close to 430 °C and close to 460 °C for [ILs.PF_6].

The type of the anion has an effect on the thermal stability of the bisimidazolium–ILs. Hexafluorophosphate and bis(trifluoromethane)sulfonimide show more than a 10 °C increase in the onset decomposition temperature compared with the halide salts. The thermal stability increases in the following order: $PF_6 > NTf_2 > Cl$.

3.2. Preparation of intercalated bentonites

3.2.1. XRD results of the intercalated bentonites

The success of intercalations was verified by measuring the increase in the basal (0 0 1) d-spacing. The X-ray diffraction pattern of Na-bentonite was compared to that of the intercalated bentonites, as illustrated in Fig. 4. It appears that the clay mineral crystallinity of bentonite was not diminished upon intercalation.

The organically modified clays were observed to have a strong reflection peak with the characteristic d-spacing distance that shifted towards smaller angles. The interlayer spacing of [ILs]–Bt clays was found to be higher than the crude bentonite clay (12.8 Å). The increase in the interlayer spacing of intercalated bentonites (approximately 6 Å) was due to the diffusion

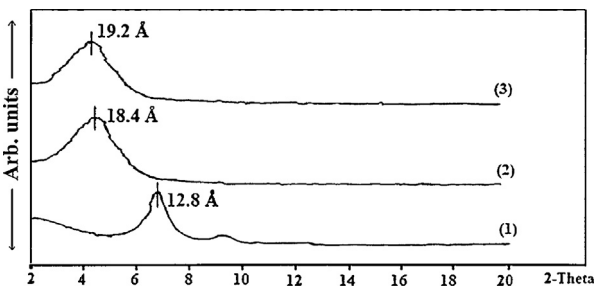

Fig. 4. XRD patterns for bentonites before and after intercalation: (0 0 1) basal peak. (1) bentonite (Bt); (2) [p.MeBIM–NTf_2]–Bt; (3) [p.MeBIM–PF_6]–Bt.

Table 1
Effect of concentration on the interlayer structure of organoclay.

Concentration (CEC of bentonite)	d_{001} (Å) [p.MeBIM–NTf_2]–Bt	d_{001} (Å) [p.MeBIM–PF_6]–Bt
1.0	14.9	15.1
2.0	18.2	19.1
3.0	18.4	19.2

of bisimidazolium-IL cations into the channels of bentonite.

Fig. 4 shows the evolution of the 0 0 1 reflection of the bentonite intercalated with [ILs.PF_6] and [ILs.NTf_2] at a bentonite concentration of 3.0 CEC. The best intercalation was obtained with [p.MeBIM–PF_6], with the d-spacing of the (0 0 1) peak shifting directly from 12.8 Å ($2\theta = 6.9°$) in the purified bentonite to 19.2 Å ($2\theta = 4.6°$) in the [ILs.PF_6]–bentonite. The spacing remained equal to 18.4 Å ($2\theta = 4.8°$) for [p.MeBIM–NTf_2]–bentonite.

Cation exchange of the sodium ion for the bisimidazolium-IL cations causes expansion of the bentonite layers. Table 1 shows the d_{001} of the organoclays prepared at different bisimidazolium-IL concentrations. Upon intercalation, the basal spacings are expanded, as expected, depending on the IL concentrations. For [p.MeBIM–NTf_2]–Bt, the d_{001} values of 1.0, 2.0 and 3.0 CEC were 14.9, 18.2 and 18.4 Å, respectively.

Table 1 clearly shows the increase in the basal spacing as the concentration of the bisimidazolium–ILs increases.

Na-bentonite hydrated moderately under room temperature conditions showed a value of 12.8 Å, and when it is modified with the [p.MeBIM–PF_6] loading of 1.0 CEC, the d-spacing value of the clay increases to 15.1 Å. This result indicated that the structural configuration of surfactant cations in the interlamellar space is a monolayer (>13.7 Å). At a concentration of 2.0 CEC and 3.0 CEC of the product, the basal spacing increases from 15.1 Å (original spacing) to 19.1 and 19.2 Å, respectively. During the excess sorption of bisimidazolium–ILs (i.e. >1.0 CEC) into the silicate layers, the transition of the cation configuration appears to occur from the monolayer to the bilayer (>17.7 Å) [25]. A previous study showed that the monolayer is formed at 13.7 Å, the bilayer at 17.7 Å, and the pseudotrimolecular at 21.7 Å, as well as the paraffin complex with basal spacings greater than 22.0 Å [26].

Depending on the layer charge (which is equal to the interlayer cation density and the packing density of the cations) of the clay mineral and the chain length of the organic ion, different arrangements of organic molecules between the layers can be formed. The geometry of the surface and the degree of exchange can also have an influence. The orientations of organic chains in clay minerals and the formation of monolayer, bilayer and pseudotrimolecular layer arrangements of organic cations in the interlayer spaces of bentonite were studied in various works [25–31].

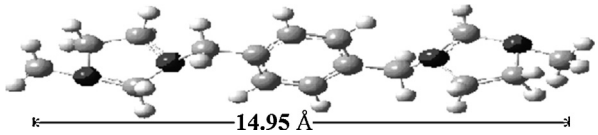

Fig. 5. Geometric calculations of bisimidazolium molecule (p.MeBIM).

The organic cations may lie flat on the silicate surface as a monolayer or bilayer, or depending on the packing density and the chain length, an inclined paraffin-type structure with the chains radiating away from the silicate surface can be formed. In the pseudotrimolecular layers, some chain ends are shifted above one another so that the spacing is determined by the thickness of three alkyl chains [27,30].

For the intercalated bentonite loading of 1.0 CEC, we observed that the interlayer spacing distance (d_{001}) is equal to the length of the molecule. The d-spacing value of clay is equal to 14.9–15.1 Å, and the geometric calculations of the bisimidazolium molecule realized after molecular modelling using Gaussian software (Fig. 5) show that the length of the molecule is approximately 14.95 Å. This result indicated that the organic cations might lie flat on the silicate surface as a monolayer and with a vertical orientation. If the molecules are lying horizontally in a monolayer, then d_{001} should be approximately equal to the width of the molecule. Even if the molecule is a cation, ion exchange will be on a monolayer. However, if the substance is organophilic and it is in excess relative to the CEC, then the first layer of the same molecules attached by ion exchange will inevitably be physically adsorbed as multilayers [27,31]. In all of these cases, d_{001} is larger than the size of the molecule.

3.2.2. *FTIR analysis of the intercalated bentonites*

The FTIR spectra of Na-bentonite (Fig. 6) reveal the presence of the characteristic absorption bands of both of the inorganic components, such as bands corresponding to Si–O, Si–O–M, and M–O–H (M = Al, Fe or Mg) that exist between anions and cations located in octahedral and tetrahedral sheets, as well as OH groups [32].

For example, bands between 3620 and 3640 cm^{-1} can be associated with the stretching vibrations of O–H groups coordinated to Al and Mg atoms (3640 cm^{-1}) or

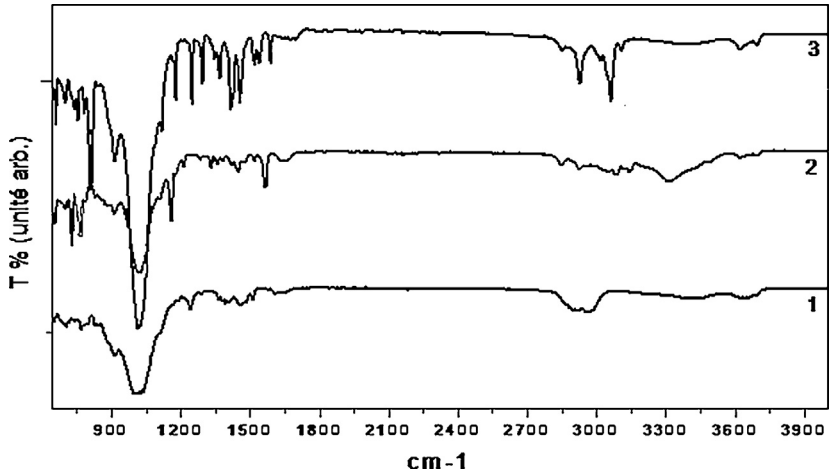

Fig. 6. FTIR spectra before and after intercalation of bentonite. (1) bentonite (Bt); (2) [p.MeBIM–NTf_2]–Bt; (3) [p.MeBIM–PF_6]–Bt.

two Al atoms (3620 cm^{-1}) in octahedral sheets of bentonite. The band centred at 1027 cm^{-1} is characteristic of the Si–O stretching vibrations. The stretching vibration bands of Si–O–M^{VI} (M = Al, Mg, and Fe) located in octahedral sheets appear over the 400–550 cm^{-1} range [33]. For M^{VI}–OH bands (M^{VI} = Al, Mg, et Fe), the Al^{VI}–OH vibrations occur at 920 cm^{-1}, and sharing of the OH group between Fe and Al in octahedral sheets can shift this peak to approximately 815–915 cm^{-1}. For our sample of bentonite, the peak appears at 913 cm^{-1}. The characteristic bands of impurities at 1034, 915, 798 and 694 cm^{-1} are manifested by shoulders attributed to the presence of quartz [34].

The FTIR spectra of the intercalated bentonites (Fig. 6) reveal the presence of characteristic absorption bands of inorganic and organic components, and the characteristic bands of the initial bentonite were unaffected (i.e., the band at 991 cm^{-1} can be associated with the Si–O stretching vibrations). Other bands, i.e., those at 734, 830, 846, 1101, 1317, 1480, 1514 and 1581 cm^{-1}, are consistent with those observed for bisimidazolium–ILs [32–34].

There is a group of absorption bands between 3420 and 3630 cm^{-1} that is due to the stretching band of the OH groups and the bending bands at 910 and 890 cm^{-1} [31]. The band at 1630 cm^{-1} also corresponds to the OH deformation of water, which allows the observation of natural bentonite and intercalated bentonites; however, the peak intensity of intercalated bentonites is lower than natural bentonite [34]. For the band at 3035 cm^{-1}, which is characteristic of aromatic C–H bonds of bisimidazolium cations and is generally of low intensity and occurs just to the left of a normal saturated C–H band, and the bands between 1450 and 1600 cm^{-1}, characteristic peaks are assigned to the stretching vibrations of the aromatic ring double bond. In addition, the bands over the 690–900 cm^{-1} range are due to C–H out-of-plane bending of aromatic products. These bands were only observed for intercalated bentonites and may provide acceptable evidence for the surface modification occurring on bentonite.

The bands only observed at 2800–2950 cm^{-1} of intercalated bentonites can be associated with the symmetric and asymmetric stretching vibrations of the methyl and methylene groups. Their bending vibrations are between 1350 and 1480 cm^{-1}, supporting the intercalation of ionic liquid molecules between the silica layers [32–34].

3.2.3. TG analysis of the intercalated bentonites

The amounts of intercalated bentonite products deduced from the TGA experiments are shown in Table 2. The mass-loss (±0.02%) was calculated from the difference between the mass-loss of the organobentonite and that of bentonite [34,35].

The mass loss from TGA and its derivative (DTG) of Na–Bt and intercalated bentonites are graphically represented in Fig. 7.

Concerning the dried bentonite curve, a 9.2% mass-loss was recorded over the temperature range of 40–200 °C, and a 4.75% mass-loss appeared from 350 to 800 °C. The first mass loss is due to desorption of water molecules, which were adsorbed onto the cations in the bentonite interlayer. The second mass loss is related to the removal of water molecules from the crystal lattice, with one alumina octahedral sheet inserted between two silica tetrahedral sheets.

Between 200 and 800 °C, CO, CO_2 and water are released in addition to Cl_2 [36]. The presence of carbon

Table 2
Percentage of intercalated product in bentonite.

Sample	Mass-loss (%)					Intercalated product (%)
	$T < 200\,^{\circ}C$	T: 200–350 °C	T: 350–500 °C	T: 500–700 °C	T: 700–800 °C	
Bentonite	9.2	0.62	1.25	3.10	0.4	–
[ILs.PF_6]	2	6	76	8	–	–
[ILs.NTf_2]	2	8	72	12	–	–
[ILs.PF_6]–Bt	9.6	4.83	13.8	3.6	2	13.26
[ILs.NTf_2]–Bt	6.2	3.61	8.46	5.9	2.4	8.86

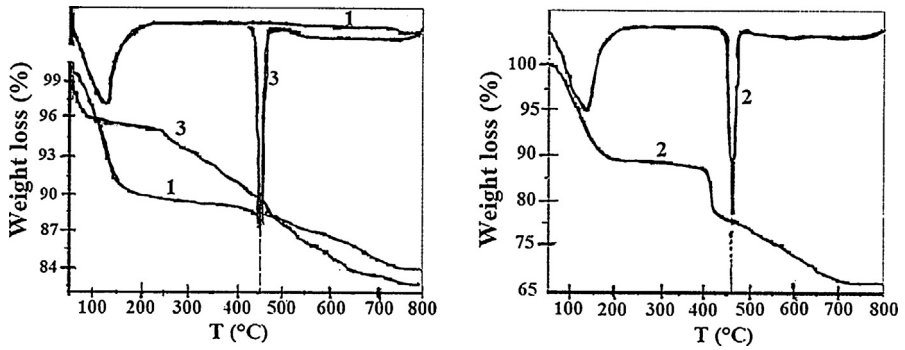

Fig. 7. TGA (DTG) curves of bentonite and intercalated bentonites. (1) bentonite; (2) [p.MeBIM–PF_6]–Bt; (3) [p.MeBIM–NTf_2]–Bt.

and sulfur is attributed to organic contamination in bentonite; sulfur is released as SO_2 at temperatures above 700 °C, and the presence of Cl is attributed to traces of NaCl in the Na-Bt. Note that the peak at 160 °C in the DTA curve corresponds to bonded water, which according to the literature, is associated with the Brönsted acid sites [37]. On the other hand, the broad and weak bands at approximately 700 °C can be assigned to the structural water released during the dehydroxylation/dehydration process [37].

Concerning the organobentonites, the mass-loss due to the presence of product in the bentonites is clearly noticed. Fig. 7 combines the TGA curves for the bentonite and organoclays investigated and shows the corresponding derivative mass-loss curves. To discuss the thermal characteristics of modified bentonites, we separated the curves into 4 distinct regions: (a) evolution of free water and gases below 200 °C; (b) evolution of organic products between 200 and 500 °C; (c) dehydroxylation of bentonite between 500 and 700 °C and (d) evolution of carbonaceous residues between 700 and 800 °C.

The thermal behaviour of the organoclays in region (b) is very important in terms of their function as nanofillers of polyolefins because it is in this temperature range that the interlayer cations begin to decompose.

The onset temperatures of degradation for organoclays are derived from the DTG curves at the point where the derivative mass-loss increases to >0.02%/°C. The DTG curves in the region between 200 and 500 °C are characterized by an exothermic peak. The temperature at the onset of the first (prominent) isotherm is taken to represent the point at which the intercalated molecules begin to decompose [21]. For the partially exchanged [ILs.PF_6]–Bt, this peak has a maximum (T_{max}) at 470 °C, and the T_{max} for [ILs.NTf_2]–Bt occurs at 450 °C, representing a downward shift of 20 °C relative to the value for [ILs.PF_6]–Bt. Therefore, it appears that the thermal stability of [ILs]-Bt decreases as the amount of intercalated surfactant increases. The onset temperatures for the bisimidazolium–ILs intercalated bentonites ([ILs.PF_6]–Bt and [ILs.NTf_2]–Bt) are close to 450–470 °C, which is significantly higher than the values for the bisimidazolium (310–380 °C) [13] or diphosphonium (300–350 °C) exchanged bentonites [14].

4. Conclusion

In this contribution, we discussed the thermal stability of several bisimidazolium salts, bisimidazolium–ILs and ionic liquid-intercalated bentonite layered silicates.

The geometric effects of synthesized bisimidazolium were discussed, and it was clearly shown that the thermal stability of the para molecules is higher than that of the meta and ortho molecules of bisimidazolium salts. In addition, the thermal stability of bisimdazolium salts is

affected by the type of isomeric structure of the alkyl side group; this is evidenced by the higher thermal stability of benzyl-BIM and butyl-BIM than dimethyl-BIM and methyl-BIM. A relationship was observed between the chain length of the alkyl group and the thermo-stability; as the chain length increased from methyl, dimethyl, butyl, to benzyl, the stability increased.

The onset temperature of the decomposition for [ILs.NTf_2] is close to 430 °C, and it is close to 460 °C for [ILs.PF_6]. The anion type affects the thermal stability, which increases in the following order: $PF_6 > TF_2 > Cl$.

Preparations of new organoclays were performed through the intercalations of bisimidazolium–ILs into the interlayer of Na-bentonite. The intercalated bentonites have a greater thermal stability (450–470 °C) compared with the halide bisimidazolium salts. These results appear to be promising in terms of the potential application of these bisimidazolium–ionic liquids for the preparation of high-temperature polymer-layered silicates.

References

[1] M.L. Patil, C.V. Laxman Rao, S. Takizawa, K. Takenaka, K. Onitsuka, H. Sasai, Synthesis of novel spiro imidazolium salts as chiral ionic liquids, Tetrahedron 63 (2007) 12702–12711.

[2] G. Mloston, J. Romanski, M. Jasinski, H. Heimgartner, Exploration of 4,5-dimethyl-1H-imidazole N-oxide derivatives in the synthesis of new achiral and chiral ionic liquids, Tetrahedron Asymmetry 20 (2009) 1073–1080.

[3] L.J. Liu, W. Feijun, M. Shi, Elimination of an alkyl group from imidazolium salts: imidazole-coordinated dinuclear monodentate NHC-palladium complexes driven by self-assembly and their application in the Heck reaction, Eur. J. Inorg. Chem. 13 (2009) 1723–1728.

[4] M. Nonnenmacher, D. Kunz, F. Rominger, T. Oeser, Palladium (II) complexes bearing methylene and ethylene bridged pyrido-annelated N-heterocyclic carbene ligands as active catalysts for Heck and Suzuki-Miyaura cross-coupling reactions, J. Organomet. Chem. 692 (2007) 2554–2563.

[5] M.Y. Pletney, Chemistry of surfactants, Stud. Interface Sci. 13 (2001) 1–97.

[6] P.C. Tsai, W.H. Ding, Determination of alkyltrimethylammonium surfactants in hair conditioners and fabric softeners by gas chromatography-mass spectrometry with electron-impact and chemical ionization, J. Chromatogr. A 1027 (2004) 103–108.

[7] M. Galinski, A. Lewandowski, I. Stepniak, Ionic liquids as electrolytes, Electrochim. Acta 51 (2006) 5567–5580.

[8] W. Kubo, T. Kitamura, K. Hanabusa, Y. Wada, S. Yanagida, Quasi-solid-state dye-sensitized solar cells using room temperature molten salts and a low molecular weight gelator, Chem. Commun. 4 (2002) 374–375.

[9] R. Martin, L. Teruel, C. Aprile, J.F. Cabeza, M. Alvaro, H. Garcia, Imidazolium ionic liquids in OLEDs: synthesis and improved electroluminescence of an ionophilic diphenylanthracene, Tetrahedron 64 (2008) 6270–6274.

[10] J. Lee, M.J. Panzer, Y. He, T.P. Lodge, C.D. Frisbie, Ion gel gated polymer thin-film transistors, J. Am. Chem. Soc. 129 (2007) 4532–4533.

[11] A. Balducci, U. Bardi, S. Caporali, M. Mastragostino, F. Soavi, Ionic liquids for hybrid supercapacitors, Electrochem. Commun. 6 (2004) 566–570.

[12] L. Weiwei, C. Lingyan, Z. Yumei, W. Huaping, Y. Mingfang, The physical properties of aqueous solution of room-temperature ionic liquids based on imidazolium: database and evaluation, J. Mol. Liq. 140 (2008) 68–72.

[13] B. Makhoukhi, D. Villemin, M.A. Didi, Preparation, characterization and thermal stability of bentonite modified with bis-imidazolium salts, Mater. Chem. Phys. 138 (2013) 199–203.

[14] B. Makhoukhi, M.A. Didi, D. Villemin, Modification of bentonite with diphosphonium salts: synthesis and characterization, Mater. Lett. 62 (2008) 2493–2496.

[15] M.A. Didi, B. Makhoukhi, A. Azzouz, D. Villemin, Colza oil bleaching through optimized acid activation of bentonite-A comparative study, Appl. Clay Sci. 42 (2009) 336–344.

[16] B. Makhoukhi, M.A. Didi, D. Villemin, A. Azzouz, Acid activation of bentonite for use as a vegetable oil bleaching agent, Int. J. Fats 60 (2009) 343–349.

[17] B. Makhoukhi, M.A. Didi, H. Moulessehoul, A. Azzouz, D. Villemin, Diphosphonium ion-exchanged montmorillonite for Telon dye removal from aqueous media, Appl. Clay Sci. 50 (2010) 354–361.

[18] B. Makhoukhi, M.A. Didi, H. Moulessehoul, A. Azzouz, Telon dye removal from Cu(II)-containing aqueous media using p-diphosphonium organo-montmorillonite, Med. J. Chem. 2 (2011) 44–55.

[19] A. Akçay, V. Balci, A. Uzun, Structural factors controlling thermal stability of imidazolium ionic liquids with1-n-butyl-3-methylimidazolium cation on Al_2O_3, Thermochim. Acta 589 (2014) 131–136.

[20] K. Noack, P.S. Schulz, N. Paape, J. Kiefer, The role of the C2 position in inter-ionic interactions of imidazolium based ionic liquids: a vibrational and NMR spectroscopic study, Phys. Chem. Chem. Phys. 12 (2010) 14153–14161.

[21] Y. Gao, L. Zhang, Y. Wang, H. Li, Probing electron density of H-bonding between cation–anion of imidazolium-based ionic liquids with different anions by vibrational spectroscopy, J. Phys. Chem. B 114 (2010) 2828–2833.

[22] M.T. Clough, K. Geyer, P.A. Hunt, J. Mertes, T. Welton, Thermal decomposition of carboxylate ionic liquids: trends and mechanisms, Phys. Chem. Chem. Phys. 15 (2013) 20480–20495.

[23] P. Pankaj, S. Arifa, A. Ishtiaque, Synthesis, surface active and thermal properties of novel imidazolium cationic monomeric surfactants, J. Ind. Eng. Chem. 20 (2014) 4267–4275.

[24] Z. Shen, G.P. Simon, Y-B. Cheng, Comparison of solution intercalation and melt intercalation of polymer-clay nanocomposites, Polymer 43 (2002) 4251–4260.

[25] X. Yunfei, D. Zhe, H. Hongping, L.F. Ray, Structure of organoclays an X-ray diffraction and thermogravimetric analysis study, J. Colloid Interface Sci. 277 (2004) 116–120.

[26] S.Y. Lee, S.J. Kim, Expansion characteristics of organoclay as a precursor to nanocomposites, Colloids Surf. A 211 (2002) 19–26.

[27] L.B. De Paiva, A.R. Morales, F.R. Valenzuela Diaz, Organoclays: properties, preparation and applications, Appl. Clay Sci. 42 (2008) 8–24.

[28] Y.C. Lee, W.K. Park, J.W. Yang, Removal of anionic metals by amino-organoclay for water treatment, J. Hazard. Mater. 190 (2011) 652–658.

[29] Y.C. Lee, E.J. Kim, D.A. Ko, J.W. Yang, Water-soluble organo-building blocks of aminoclay as a soil-flushing agent for heavy metal contaminated soil, J. Hazard. Mater. 196 (2011) 101–108.
[30] G. Lagaly, Characterization of clays by organic compounds, Clay Miner. 16 (1981) 1–21.
[31] G. Lagaly, M.F. Gonzalez, A. Weiss, Problems in layer-charge determination of montmorillonites, Clay Miner. 11 (1976) 173–187.
[32] B. Makhoukhi, M. Djab, M.A. Didi, Adsorption of Telon dyes onto bis-imidazolium modified bentonite in aqueous solutions, J. Environ. Chem. Eng. 3 (2015) 1384–1392.
[33] M.S. Lakshmi, B. Narmadha, B.S.R. Reddy, Enhanced thermal stability and structural characteristics of different MMT-Clay/epoxy-nanocomposite materials, Polym. Degrad. Stab. 93 (2008) 201–213.
[34] L. Le Pluart, J. Duchet, H. Sautereau, J.F. Gerard, Surface modifications of montmorillonite for tailored interfaces in nanocomposites, J. Adhes. 78 (2002) 645–662.
[35] J.Y. Lee, H.K. Lee, Characterization of organobentonite used for polymer nanocomposites, Mater. Chem. Phys. 85 (2004) 410–415.
[36] A. Azzouz, D. Messad, D. Nistor, C. Catrinescu, A. Zvolinschi, S. Asaftei, Vapor phase aldol condensation over fully ion-exchanged montmorillonite-rich catalysts, Appl. Catal. A 6390 (2002) 1–13.
[37] H.A. Patel, R.S. Somani, H.C. Bajaj, R.V. Jasra, Preparation and characterization of phosphonium montmorillonite with enhanced thermal stability, Appl. Clay Sci. 35 (2007) 194–200.